Journal of Applied Remote Sensing

RemoteSensing.SPIEDigitalLibrary.org

Use of shadow for enhancing mapping of perennial desert plants from high-spatial resolution multispectral and panchromatic satellite imagery

Saad A. Alsharrah
Rachid Bouabid
David A. Bruce
Sekhar Somenahalli
Paul A. Corcoran

SPIE.

Saad A. Alsharrah, Rachid Bouabid, David A. Bruce, Sekhar Somenahalli, Paul A. Corcoran, "Use of shadow for enhancing mapping of perennial desert plants from high-spatial resolution multispectral and panchromatic satellite imagery," *J. Appl. Remote Sens.* **10**(3), 036008 (2016), doi: 10.1117/1.JRS.10.036008.

Use of shadow for enhancing mapping of perennial desert plants from high-spatial resolution multispectral and panchromatic satellite imagery

Saad A. Alsharrah,[a,*] Rachid Bouabid,[b] David A. Bruce,[a] Sekhar Somenahalli,[a] and Paul A. Corcoran[a]

[a]University of South Australia, School of Natural and Built Environments Research Centre, GPO Box 2471, Adelaide, Australia

[b]Ecole Nationale d'Agriculture de Meknes, Km 10, Rte Haj Kaddour, BP S-40 Meknès 50000, Morocco

Abstract. Satellite remote-sensing techniques face challenges in extracting vegetation-cover information in desert environments. The limitations in detection are attributed to three major factors: (1) soil background effect, (2) distribution and structure of perennial desert vegetation, and (3) tradeoff between spatial and spectral resolutions of the satellite sensor. In this study, a modified vegetation shadow model (VSM-2) is proposed, which utilizes vegetation shadow as a contextual classifier to counter the limiting factors. Pleiades high spatial resolution, multispectral (2 m), and panchromatic (0.5 m) images were utilized to map small and scattered perennial arid shrubs and trees. We investigated the VSM-2 method in addition to conventional techniques, such as vegetation indices and prebuilt object-based image analysis. The success of each approach was evaluated using a root sum square error metric, which incorporated field data as control and three error metrics related to commission, omission, and percent cover. Results of the VSM-2 revealed significant improvements in perennial vegetation cover and distribution accuracy compared with the other techniques and its predecessor VSM-1. Findings demonstrated that the VSM-2 approach, using high-spatial resolution imagery, can be employed to provide a more accurate representation of perennial arid vegetation and, consequently, should be considered in assessments of desertification. [DOI: 10.1117/1.JRS.10.036008]

Keywords: desertification; perennial; vegetation; classification; shadow; object based.

Paper 15896P received Dec. 23, 2015; accepted for publication Jul. 7, 2016; published online Jul. 22, 2016.

1 Introduction

Desertification has raised major global concerns in recent years due to its contribution to losses in biodiversity, soil erosion, and agricultural production.[1] The limitation of land productivity is particularly alarming as it intensifies poverty and political instability. Use of remote sensing to assess and monitor desertification creates avenues for cost-effective methods to evaluate biophysical indicators in the context of desert environments with very scattered vegetation. Moreover, the temporal resolution of remote sensing provides an invaluable attribute for analyzing desertification trends by investigating changes in vegetation cover across time.[2] However, the current approach of applying regional scale ($<400 \times 400$ km) and lower spatial resolution satellite imagery (30 to 250 m) for assessing desertification is arguably concerning, due to the structural characteristics and distribution of perennial arid vegetation. Perennial arid vegetation is often relatively small in size (0.4 to 4 m in diameter), exhibits sparse distribution and such assessments may weaken the confidence of researchers in their ability to retrieve adequate information on vegetation cover.[3] Furthermore, the heterogeneity of arid landscapes (mainly soils) is a fundamental characteristic and should be taken into account when mapping perennial

*Address all correspondence to: Saad A. Alsharrah, E-mail: saad.al-sharrah@mymail.unisa.edu.au

1931-3195/2016/$25.00 © 2016 SPIE

vegetation cover. These considerations encourage the use of higher spatial resolution satellite imagery (submeter to 5 m) to extract perennial vegetation-cover information at the local scale.

Remote-sensing methods, such as vegetation indices (VIs), can provide an estimate of the greenness of an area as they are sensitive to vegetation cover.[4] However, the classical VIs approach entails challenges when attempting to detect arid vegetation due to the dominance of soil background within each pixel, which makes it difficult to retrieve accurate quantitative information on vegetation cover.[5] In addition to VIs, other remote-sensing techniques, such as spectral mixture analysis (SMA), have been applied successfully for detecting vegetation cover in arid lands.[6–8] SMA, however, is optimum when using satellite imagery that incorporates a large number of spectral bands. Currently, high-spectral resolution satellite sensors often exhibit low-spatial resolution and hence the tradeoff between resolutions is an important issue.[9] The use of VIs and SMA are the preferred approaches when handling pixels that are usually larger (in size) than the object of interest.[10] VIs, however, still dominate researchers' and stakeholders' preferences due to their relative simplicity in comparison to the more complex SMA. Notably, a number of studies[11,12] have focused on applying SMA to high-spatial resolution imagery and found success in their approach. Although these studies provide a valid and worthy avenue of inquiry, especially with the availability of more spectral bands, it is not pursued in this study due to the focus of generating an operational approach for efficient delineation of perennial arid vegetation.

There is an increasing interest in integrating other variables, such as texture and context, to enhance the mapping process of target objects in the field of remote sensing.[13,14] Although the use of spatial properties to distinguish between features is applied mostly during visual interpretation, increased interest grew concurrently with the emergence of high-spatial resolution satellites in the recent years.[15] This has led to the movement toward the use of object-based image analysis (OBIA), which is based on segmenting the image into relatively homogeneous regions using the size, shape, texture, and context associated with the regions, thus providing an improved basis for image analysis.[16] Unlike the traditional pixel-based approaches, OBIA combines spectral and contextual information to classify objects that consist of a few pixels.[16] The rise of commercially available high-spatial resolution satellite imagery (<5 m) and the ever-growing availability of powerful off-the-shelf software invites investigation of the potentiality for mapping perennial arid shrubs and trees at high levels of accuracy. Advancement in this field can provide encouragement to shift away from the recognized limitations of pixel-based remote-sensing methods, which fail to represent true geographical objects and entail limited pixel topology. For desertification assessment and monitoring, semiautomated OBIA for vegetation classification would be an advance. However, challenges still remain even with higher spatial resolution imagery, where the usually square pixel in images may not faithfully relate to the geometric characteristics of arid shrubs and trees. Therefore, a more precise delineation of perennial arid shrubs and trees using a semiautomatic workflow can potentially provide invaluable information to arid land managers and potentially be used as accuracy assessors for the current assessment, monitoring, and modeling practices, which employ low- to medium-spatial resolution data. In the near future, with growing archives of high-spatial resolution imagery, development of operational and automatic or semiautomatic biophysical information extraction methods are necessary to feed an array of applications and stakeholders that can benefit from this vital information.

This study builds on the vegetation shadow model (VSM-1),[17] which used shadow as a contextual reclassifier that acted as a clean-up operator for an overclassified vegetation-cover image derived from VIs. The objective of this study was to evaluate the ability of an extended vegetation shadow model (VSM-2) that takes into account vegetation size and structure to enhance the accuracy of vegetation-cover extraction in arid environments at a local scale, with comparisons to results from VIs, prebuilt OBIA and its predecessor VSM-1. The primary focus was on perennial shrubs and small trees that are key in stabilizing the soil, rather than on seasonal short grasses.

2 Materials and Methods

2.1 *Study Area and Satellite Imagery*

The study area for this reserach was located in the central arid and semiarid lands of the Meknes–Tafilalet region in north central Morocco (Fig. 1) between latitudes 32.869°N and 32.959°N and

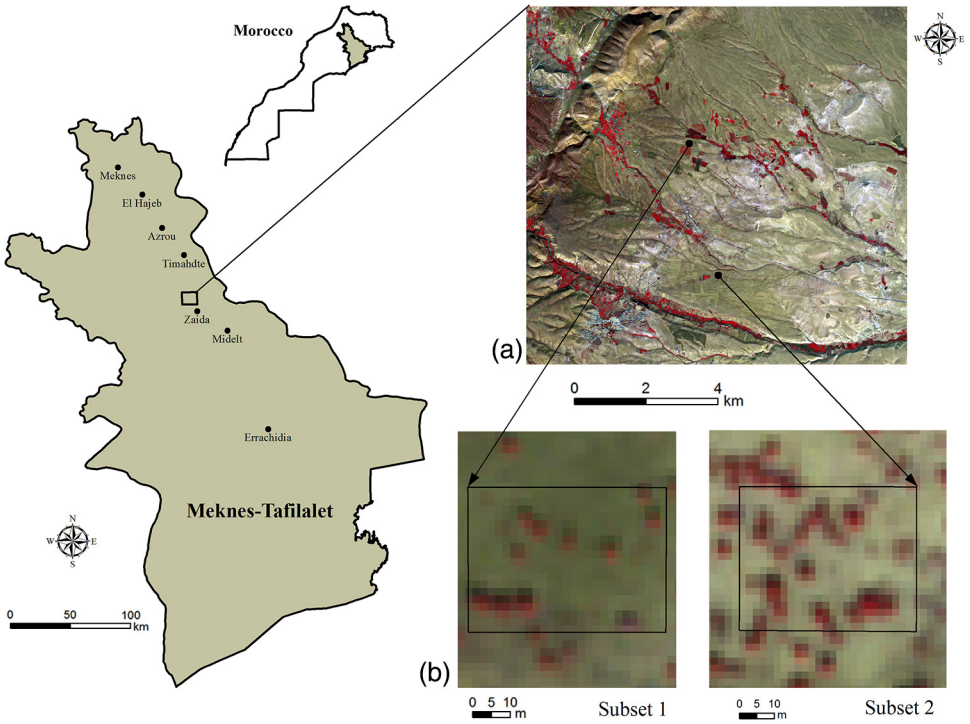

Fig. 1 (a) Study area extent Pleiades 1A Image (RGB—4, 3, 2). (b) Two subsets of the study area.

longitudes 4.964°W to 5.077°W. The choice of the study area was motivated by the evident and current land degradation processes and the lack of rigorous assessment in these particular areas. The region contians many rural communities and small villages that are primarily affected by the desertification process. The study area, which encompasses an amalgamation of various dryland subtypes such as semiarid mountainous, semiarid and arid regions, is a transition between the Atlas mountains piedmonts and the harsher sub-Sahara of south-eastern Morocco. Land cover within the study area supports mixed grazing and agricultural practices in a diagonal (NW to SE) spatial distribution, which is associated with the flow of natural, intermittent water courses. The area is very dry; rainfall (less than 200 mm/year) is infrequent and erratic and desert winds can be extremely strong. In this study, two subsets (dominated by *Artiplex Halimus* and *Retama Monosperma*) covering 50 m × 40 m were selected from the study area. Subset 1 represents a microdesert ecosystem with sparsely distributed desert vegetation and high-soil background reflectance, whereas Subset 2 is a more densely vegetated area with larger vegetation structural characteristics and a lower soil background area. Both subsets were selected based on consultation with local expert desert ecologists, the experience from a field visit conducted in 2012 and visual interpretation of high-spatial resolution satellite imagery.

Field data collection was conducted in November 2013 to assess the performance of the VIs and the OBIA approaches applied to the imagery over the two subsets. The field study involved using a Leica SR 530 differential GPS (dGPS) to collect positions of perennial shrubs and trees to ~10-cm accuracy. For each subset, measurements of the physical characteristics of the target objects, including height and canopy diameter, were conducted. The sampling strategy collected information on all present vegetation (perennial shrubs and small trees) within the subsets that had an approximate canopy diameter of 50 cm and above, based on the rationale that plants larger than this size are key in supporting root systems and stabilizing soil structures.

A high-spatial resolution multispectral Pleiades 1A image was acquired dated November 15, 2012 during the autumn season when the perennial vegetation is dominant. Ground sampling distance (approximately the spatial resolution) of the image was 2 m with four spectral bands including blue (0.43 to 0.55 μm), green (0.50 to 0.62 μm), red (0.59 to 0.71 μm) and near-infrared (0.74 to 0.94 μm). The image was geometrically corrected and ortho-rectified to UTM 30N WGS84. Radiometric calibration was applied using the ATCOR 2 model, which implements the MODTRAN4+ radiative transfer code.[18]

2.2 *Ground Truth and Accuracy Assessments*

Traditional accuracy assessment approaches in the classification of vegetation cover predominantly use percent cover as the solitary means of assessment.[19–21] Percent cover was embraced in this study as one assessment parameter. Therefore, percent cover relative to the investigated subsets was derived from estimates generated from the remote-sensing mapping method. The assessment parameter was further supplemented with commission and omission errors to develop an evaluation metric to assess the performance of the different perennial vegetation-cover extraction approaches (Fig. 2).

To evaluate the performance of a remote-sensing method for mapping individual shrubs and trees, it is not sufficient to utilize just percent cover as the sole mean of assessment. Various weaknesses are inherent with such an approach. For example, a method resulting in overclassification of a certain patch of vegetation can complement cover estimates from patches that were not detected (under classification). For high-accuracy delineation of individual shrubs and trees, metrics such as commission and omission, which are rarely used in arid vegetation studies, can assist in evaluating how accurately the methods map vegetation. Employment of commission and omission errors is widespread in forest inventory studies, where these metrics are applied to classical confusion matrices to evaluate the methods' performance in detecting individual tree crowns.[22,23] Following the generation of vegetation-cover estimates, the performance of each approach was evaluated and assessed using the developed root sum square (RSS) error metric

$$\mathrm{RSS} = \sqrt{(1-\mathrm{CE})^2 + (1-\mathrm{OE})^2 + (1-\mathrm{PCE})^2}, \tag{1}$$

where

$$\text{Commission error (CE)} = 1 + \frac{\text{Commission area}}{\text{Truth area}}, \tag{2}$$

$$\text{Omission error (OE)} = 1 + \frac{\text{Omission area}}{\text{Truth area}}, \tag{3}$$

$$\text{Percent cover error (PCE)} = \frac{\text{Percent cover}}{\text{True percent cover}}. \tag{4}$$

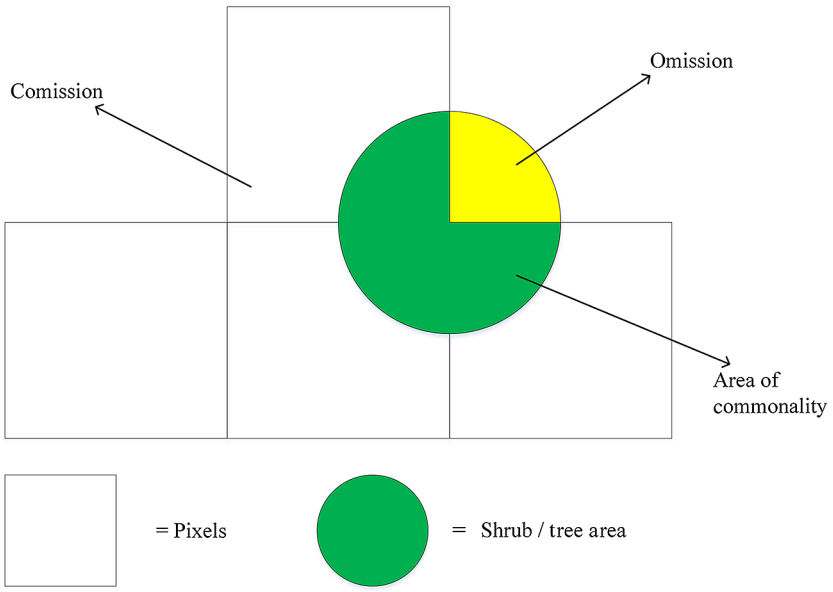

Fig. 2 Schematic diagram delineating the inputs used in the RSS metric.

Geographic information systems (GIS) analysis was utilized to extract percent cover area, commission area and omission area for each perennial vegetation-cover output. Using a vector intersect operation between the derived cover area and the "true" cover area, as defined by the dGPS position of each shrub or tree plus field measurement of canopy diameter, an area of commonality was generated and was further used to identify the area of omission. An erase operation was applied on the vectorized boundaries of the derived vegetation cells using the true perennial vegetation cover to calculate the area of omission. Percent cover of each output was extracted using the statistics tool in the GIS. The calculations of the errors returned metrics, where best performance was with values closer to 1 for the individual metrics of CE, OE, and PCE. Following the generation of perennial vegetation-cover estimates, the performance of each approach was evaluated and assessed using the RSS, where a value closer to 0 was best.

2.3 *Vegetation Indices Threshold Analysis*

While VIs analysis has been undertaken before, it was included in this study because of its extensive use and acceptance for mapping arid vegetation in desertification studies due to its simplicity and efficiency, and to assess the sensitivity of mapping accuracy with variation in index thresholds. The indices utilized included the normalized vegetation index (NDVI),[24] soil-adjusted vegetation index (SAVI),[25] modified soil-adjusted vegetation index 2 (MSAVI-2),[26] transformed soil-adjusted vegetation index (TSAVI-2),[27] perpendicular vegetation index 1 (PVI-1),[28] perpendicular vegetation index 3 (PVI-3),[26] and perpendicular distance 54 (PD-54).[29] Image processing software ERDAS IMAGINE 2015[30] was used to calculate the VIs where prebuilt indices in the software were utilized for automatic extraction (NDVI, SAVI, and MSAVI-2). Other nonintegrated indices (TSAVI-2, PVI-1, PVI-3 and PD-54) were built in the Modeller function in IMAGINE. VIs were calculated using the following processes:

- SAVI was calculated with differing L values of 0.5, 0.75, and 1.0.
- TSAVI-2, PVI-1, and PVI-3 were calculated by first deriving the slope and intercept of the soil line in an NIR and R scatterplot for the whole image (slope = 1.0682 and the intercept = 0.099).
- Dry and moist soil data points were used to generate soil-line data and to extract the values.
- For PD-54, the slope and intercept were extracted from the soil line in a green (G) and R scatterplot for the whole image (slope = 1.317 and the intercept = 0.0569).

The literature on the application of VIs for extracting vegetation cover acknowledges the inherent issue of threshold selection and its role in over or underclassification.[19] However, commission and omission errors and their effects on the classification output are rarely discussed in arid zone studies. Moreover, results from VIs provide a good starting point and a benchmark for comparison with the subsequent remote-sensing methods employed in this study. For this study, threshold analysis was applied over the seven VIs to identify at which threshold value an optimum vegetation-cover classification for each index was returned. The selection of the range of values on which the threshold divisions were set was decided through an iterative process, where each vegetation index was examined through visual interpretation of the imagery to identify at which threshold the index returned 0% vegetation and 100% vegetation. Hence, this range provided a preparatory scale for the more detailed numerical examination of each index.

2.4 *Object-Based Image Analysis*

OBIA has gained increased interest due to the need of improved algorithms that take into account the spectral characteristics of the surrounding (contextual) pixels and also geometric and textural information of the target feature or pixel.[31] Incorporating textural information became advantageous as the spatial resolution of imagery increased.[16] Furthermore, it was a primary aim to convert pixels into image objects to eliminate the "salt and pepper effect" often caused by per-pixel classifiers. The literature on the use of OBIA for vegetation mapping shows dominance in the application to forest ecosystems.[16,32–36] However, various studies that employed OBIA for mapping arid vegetation have demonstrated promising success.[12,13,37–39] The promising, yet seemingly under researched area of mapping arid vegetation using OBIA, encourages continued

research for the development of semiautomatic and highly accurate delineation of arid shrubs and trees. With powerful commercial software, such as eCognition, IMAGINE Objective, and ENVI feature extraction, evaluating the enhancement OBIA can bring to the detection of perennial arid vegetation is a promising research area with potentially higher accuracies than traditional methods.

2.4.1 *Prebuilt object-based image analysis*

IMAGINE Objective[30] and eCognition[40] software was evaluated for mapping arid shrub and tree objects for the two subsets. IMAGINE Objective incorporates a model consisting of operators working systematically in two separate machine learning domains, raster and vector. The software uses cue algorithms that yield metrics quantified to color/tone, texture, size, shape, shadow, site/situation, pattern and association, which are measured in the raster- and vector-level learning components.[30] In IMAGINE Objective, training polygons of a feature of interest (shrubs and trees) were digitized and submitted to compute the pixel cue metrics with background pixels including grass, bare soil, shadow, buildings, and roads. Subsequently, both the embedded Segmentation and Threshold and Clump approaches were trialed. IMAGINE Objective segmentation retained significant undersegmentation, partitioning the image into large segments that did not represent the target objects. Based on these results, there was little encouragement to proceed with the consequent operators. The Threshold and Clump approach was employed which applied a threshold on a pixel probability layer, retaining pixels that have a probability greater than or equal to the threshold value. The operator converted these remaining pixels to binary (0, 1), then performed a contiguity operation (clump) on the binary values of 1. A probability threshold value of 0.9 was chosen based on visual inspection of the results from trialing the range of thresholds available from the software.

The software eCognition, with the capability of multiresolution segmentation, has been used to detect arid shrubs and often advocated to generate superior results to other remote-sensing methods.[13,37,39] The approach embedded within eCognition segments the image based on three parameters: (1) scale, (2) colour/spectra, and (3) shape. The scale is a unitless parameter which drives the size of image objects, where a larger scale parameter results in larger image objects and smaller scale parameter results in a smaller image. The color and shape parameters can be weighted from 0 to 1. Within the shape setting, smoothness or compactness can be defined and are additionally weighted from 0 to 1.[39,41] Table 1 demonstrates the segmentation parameters that were applied to Subsets 1 and 2 within the study area.

The parameters were determined based on visual inspection of the segmentation results across a range of scales and their ability in detecting shrub and tree objects. The scale of 3 was applied for the first level (level 1) of segmentation to identify shrubs and trees. A scale of 10 was used for the second level (level 2) of segmentation to investigate the potential of detecting vegetation patches as often is conducted in landscape analysis studies using multiresolution segmentation.[42,43] It must be noted that the scale of investigation in this paper is focused at the individual shrub and tree level. Therefore, a multiscale segmentation approach is not required, because other scales of landscape classes are beyond the scope of this study. Once the segmentation was complete, the classification was performed by manually training the segmented objects. Two classes were used in this analysis: (1) vegetation and (2) background.

2.4.2 *Vegetation shadow model*

The first version of VSM, known as VSM-1, used a filter to convolve the shadow pixels to colocate with their associated vegetation pixels. The concept of the VSM-1 was to apply a filter

Table 1 Segmentation parameters in eCognition.

Level	Scale	Color	Shape	Smoothness	Compactness
1	3	0.8	0.2	0.8	0.2
2	10	0.8	0.2	0.4	0.6

for the convolution of shadow pixels for the purpose of superimposing these pixels on top of associated vegetation pixels to act as a "determent of shrub/tree presence." Classification of shadow was first achieved by using a multinetwork Bayesian classifier embedded in IMAGINE Objective applied on the Pleiades panchromatic image. VIs were subsequently applied to the Pleiades multispectral image to generate a vegetation-cover image. VSM-1 generated a vegetation-cover image by applying a low-threshold NDVI (0.2) to intentionally produce an overclassified vegetation-cover raster. The raster was then resampled to 0.5-m spatial resolution to match the resolution of the shadow raster. The subsequent process was to convolve the shadow pixels and generate a convolved shadow raster. During the filter design stage, factors such as Sun azimuth and elevation at the time of image acquisition and tree structure affected the design. For this study, shadow distance (D) was calculated using the expression $D = H \cot a$ deg for some of the shrubs and trees within the study area, where H is the height of the tree and a deg is Sun elevation angle (Fig. 3). This assumes that the ground is flat, the trees are vertical, and that tree canopy does not obscure shadow. The shrubs and trees had an average height of ~1 m and an average shadow distance of ~1.3 m for the date, geographic location, and time of acquisition for the Pleiades satellite image. For these shrubs and trees, at least three pixels of 0.5-m size were needed to map and convolve their shadows.

A 3×11 filter (Fig. 4) was initially used to provide a cushion of two extra pixel to allow for higher trees and to accommodate for the grid azimuth of the shadow for the filter (-14.52 deg). Grid azimuth was computed from geographic north by application of the map projection grid convergence.

The VSM-1 model was further modified into VSM-2 by integration of multiple filters to take into account the varying sizes of perennial shrubs and trees (Fig. 5). The results of VSM-1 demonstrated that Subsets 1 and 2 yielded different levels of accuracy when utilizing the 3×11 filter due to the different structural characteristics between them. The 3×11 filter returned high errors of commission for Subset 1, especially for small-sized shrubs. More discussion regarding these results is provided in the results section. VSM-2 integrated three convolution filters that were designed to detect small-, medium-, and large-sized shrubs and trees. The model ran three convolution filters of size 3×7, 3×9, and 3×11 (Fig. 4), where the allocation of three pixels for the width of the filter was sufficient due to the shadow-grid azimuth angle (-14.52 deg). Using filter heights of 7, 9, and 11 pixels aided in detecting different sized shrubs and trees where a smaller filter is better suited to detect smaller shrubs and trees with a minimal number of shadow pixels. The model generated three convolved shadow rasters, which were also combined with the low-threshold NDVI image using a Boolean AND operation to generate three Boolean AND rasters. The three Boolean output rasters were then converted into GIS vector data and further processed to produce three vector layers that were related to small-, medium-, and large-sized

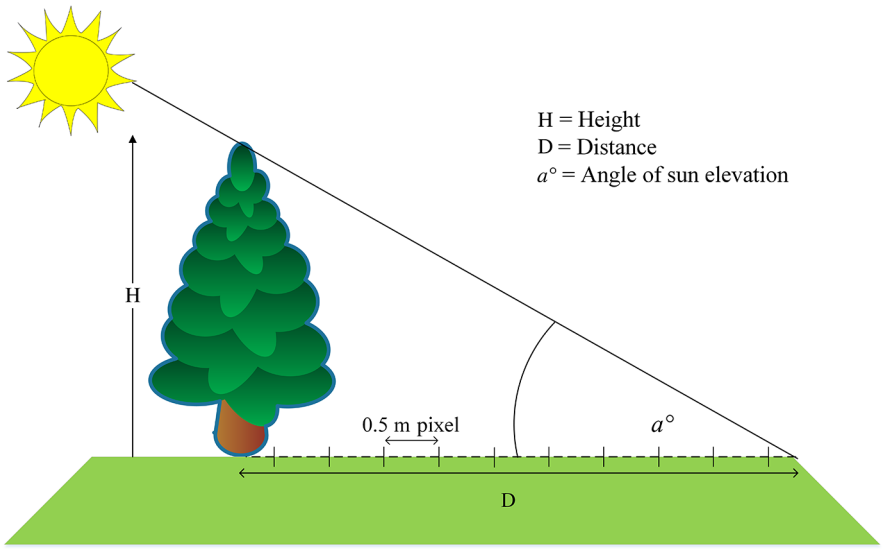

Fig. 3 Schematic diagram delineating calculation of shadow distance cast by a shrub or tree.

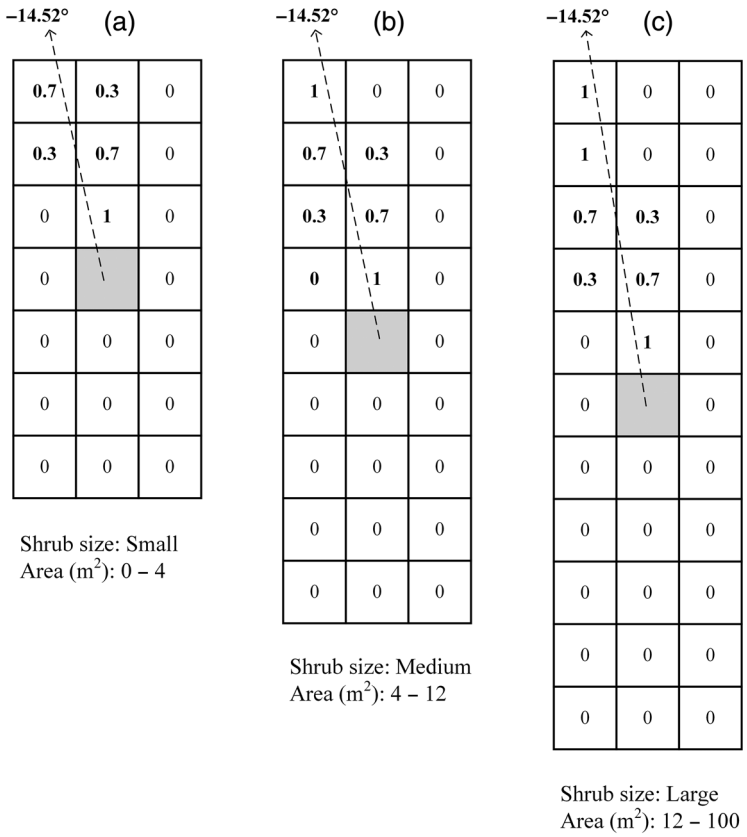

Fig. 4 Convolution filters: (a) 3×7, (b) 3×9, and (c) 3×11.

shrubs. GIS processing within the model utilized attribute queries which classified the perennial vegetation into three different shrub and tree sizes based on area. The classifications are detailed in Fig. 4. Using GIS selection queries, the model subsequently returned each class to its corresponding layer to avoid duplication of perennial vegetation-cover estimates from the multiple filters.

An allocation of 4 m^2 for small shrubs was based on the minimum possible area for the resolution of the Pleiades multispectral image of 2 m. Medium shrub area was classed between 4 and 12 m^2, whereas large shrubs were greater than 12 m^2 and up to 100 m^2. Although the focus of this study was to detect scattered low-lying shrubs and trees in arid lands, the use of up to 100 m^2 for the area of large-sized shrubs and trees was to take into account some of the vegetation clumps and interconnected perennial vegetation canopies. Classification of size was based partially on an arbitrary decision from an iterative procedure conducted through the examination of the best results and knowledge obtained from field work. It is, however, noted that further investigation of size classification mechanisms is needed and should be considered in further research. In this study, a general classification was utilized to assess whether the multi-filter approach could achieve enhancements in perennial vegetation-cover estimation and add complementary size classification information to the output. To generate a single perennial vegetation dataset, the three vectors layers were combined using a GIS union operation and dissolved to produce a perennial vegetation-cover layer.

3 Results and Discussion

The RSS metric results for VIs and OBIA are detailed in Table 2. For VIs, MSAVI-2 performed best statistically for Subset 1, an area with a higher soil background cover and small- to medium-scattered desert shrubs, where it returned an RSS of 0.738. NDVI on the other hand returned the best results for Subset 2, which is an area exhibiting denser vegetation and incorporating less soil

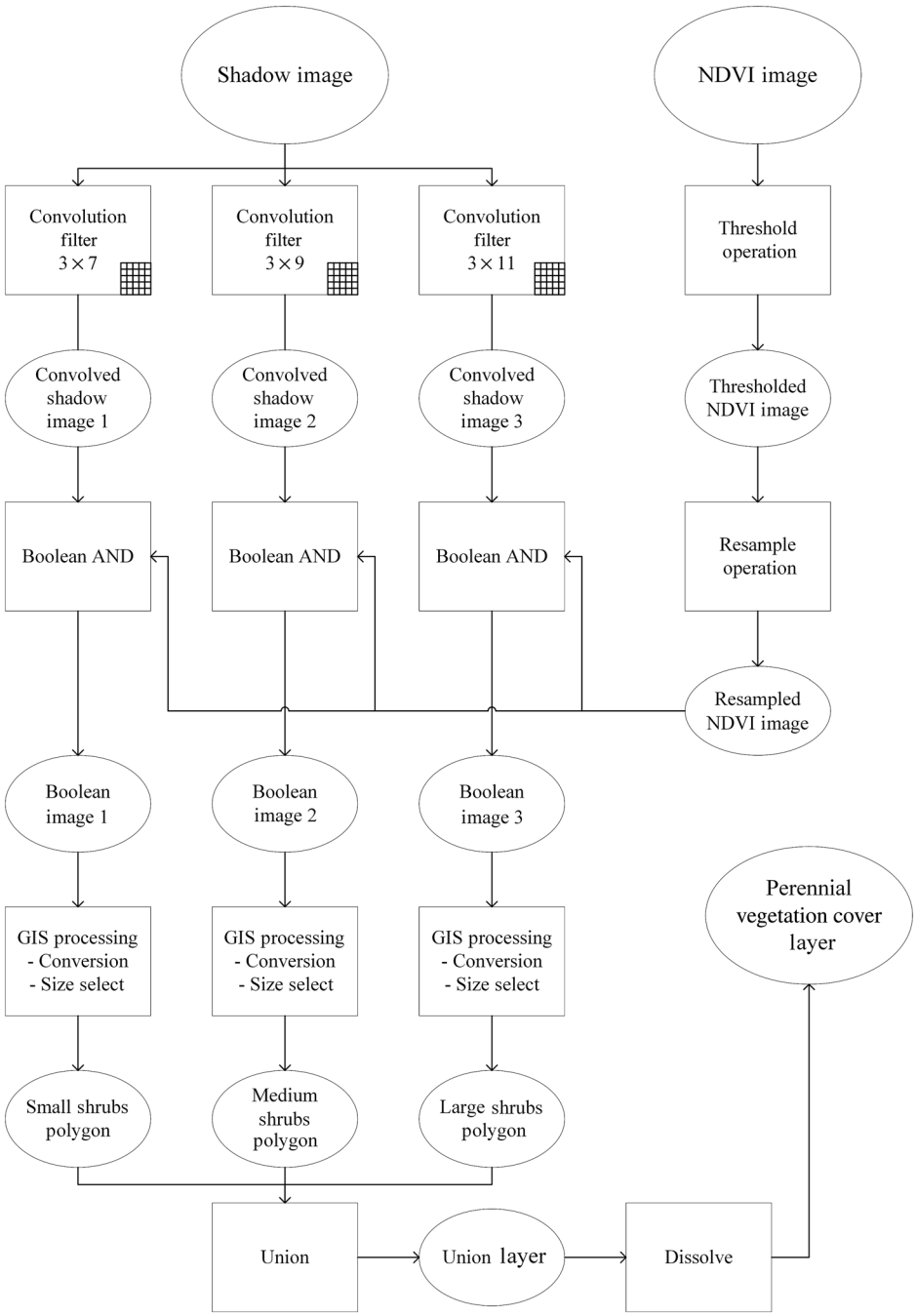

Fig. 5 VSM-2 operations and workflow.

background, with an RSS of 0.64. The IMAGINE Objective Engine did not return significant improvement compared with VIs. Based on visual inspection, it was identified that distributional accuracy was improved for both subsets, but this came with a cost of overclassification. Based on visual interpretation, the results of image segmentation using eCognition demonstrated promising signs in mapping the distribution of perennial arid shrubs and trees. Defining the scale of segmentation aided in reducing the issue of undersegmentation that was demonstrated with IMAGINE Objective, and potential to detect vegetation patches and other classes such as agriculture and bare soil. However, mapping individual perennial shrubs and trees was still limited using eCognition, especially for the target size of interest (0.5 to 2 m diameter). The limitation is largely associated with pixel size, where for perennial shrubs the size of one Pleiades multispectral pixel (2 m) will only depend on one parameter and that is the spectra of the pixel. Therefore,

Table 2 RSS for VIs and OBIA for Subsets 1 and 2.

Method	Subset 1		Subset 2	
Vegetation index	Threshold	RSS	Threshold	RSS
NDVI	0.31	0.746	0.3	0.64
SAVI ($L = 0.5$)	0.25	0.746	0.25	0.647
SAVI ($L = 0.75$)	0.24	0.739	0.24	0.65
SAVI ($L = 1$)	0.24	0.756	0.24	0.647
MSAVI2	0.24	0.738	0.24	0.657
TSAVI	0.11	0.739	0.12	0.65
PVI-1	0.21	0.759	0.22	0.788
PVI-3	0.89	0.816	0.87	0.687
PD-54	0.6	0.784	0.6	0.665
OBIA	**RSS**		**RSS**	
IMAGINE Objective Threshold and Clump	6.57		3.127	
IMAGINE Objective Threshold and Clump with Shadow Association	7.135		2.82	
VSM-1	1.498		0.542	
VSM-2	1.415		0.507	

other OBIA cues such as texture and smoothness, cannot function in identifying the objects. As a consequence, assessing cover estimates using the RSS for eCognition was not pursued. VSM-1, on the other hand, returned contrasting results, where it failed to return improved estimates statistically for Subset 1, but proved to be the optimum approach compared to the previous methods with an RSS of 0.542 for Subset 2. VSM-2 was able to further improve the results with an RSS of 1.415 and 0.507 for Subsets 1 and 2, respectively.

VIs that take into account soil reflectance such as MSAVI-2 gave the best results for Subset 1 compared with the other indices, whereas NDVI proved to have outperformed the other indices for Subset 2. This is due to the incorporation of commission errors, which tend to balance the omission areas at certain thresholds and hence return a close measure to the true total area—the percent cover. OBIA using IMAGINE Objective Engine was able to provide better distributional accuracy for Subset 1, but this came with the cost of overclassification, hence higher RSS values. The key aspect of this approach is pixel training and the associated operator skill of separating grasses and dark soils from shrubs when performing the training. VSM-1 proved to deliver improved results statistically for Subset 2 compared to the previous methods. Visual interpretation also demonstrated that for Subset 2, VSM-1 outperformed the previous approaches as it returned a high accuracy of vegetation distribution and a closer representation of the ground control (Fig. 6). However, the vegetation size and the employed filter size contributed to the lower accuracy of the results in Subset 1. VSM-1 for Subset 1 demonstrated significant visual improvement, but the RSS did not support such a conclusion. The large RSS of VSM-1 for Subset 1 is a result of a high-percent cover return (9.3%) compared with the true percent cover (4.7%). In addition, the commission area is $\sim$100 m^2 contributing to a higher RSS value of 1.498 than what was expected. We tried to resolve this performance issue by introducing multiple filters with VSM-2. The results revealed improvements for both Subsets 1 and 2 with a drop of the RSS values. Although the RSS for Subset 1 decreased in comparison to the previous study,[17] it was yet to register a lower value in comparison to VIs. This can be attributed to various factors: (1) optimum VIs thresholds take advantage of the committed areas that complement the

omitted areas which return a close measure of the true percent cover; (2) VSM-2 not only improves the distributional accuracy by detecting smaller plants but also increases the commission errors especially in areas with very small shrubs; and (3) ground truth in this study collected individual tree information and in the case of some interconnected clumps of perennial vegetation, the ground truth may underestimate the vegetation cover. An avenue of improvement to counter these limitations is the integration of an error metric for distributional accuracy. Visual interpretation confirms the improvements presented by VSM-2, evaluating the distribution and incorporating it in the RSS may also return the statistical confidence to support such conclusion. In this context, spatial statistics tools such as nearest neighbor and point clustering could be useful.

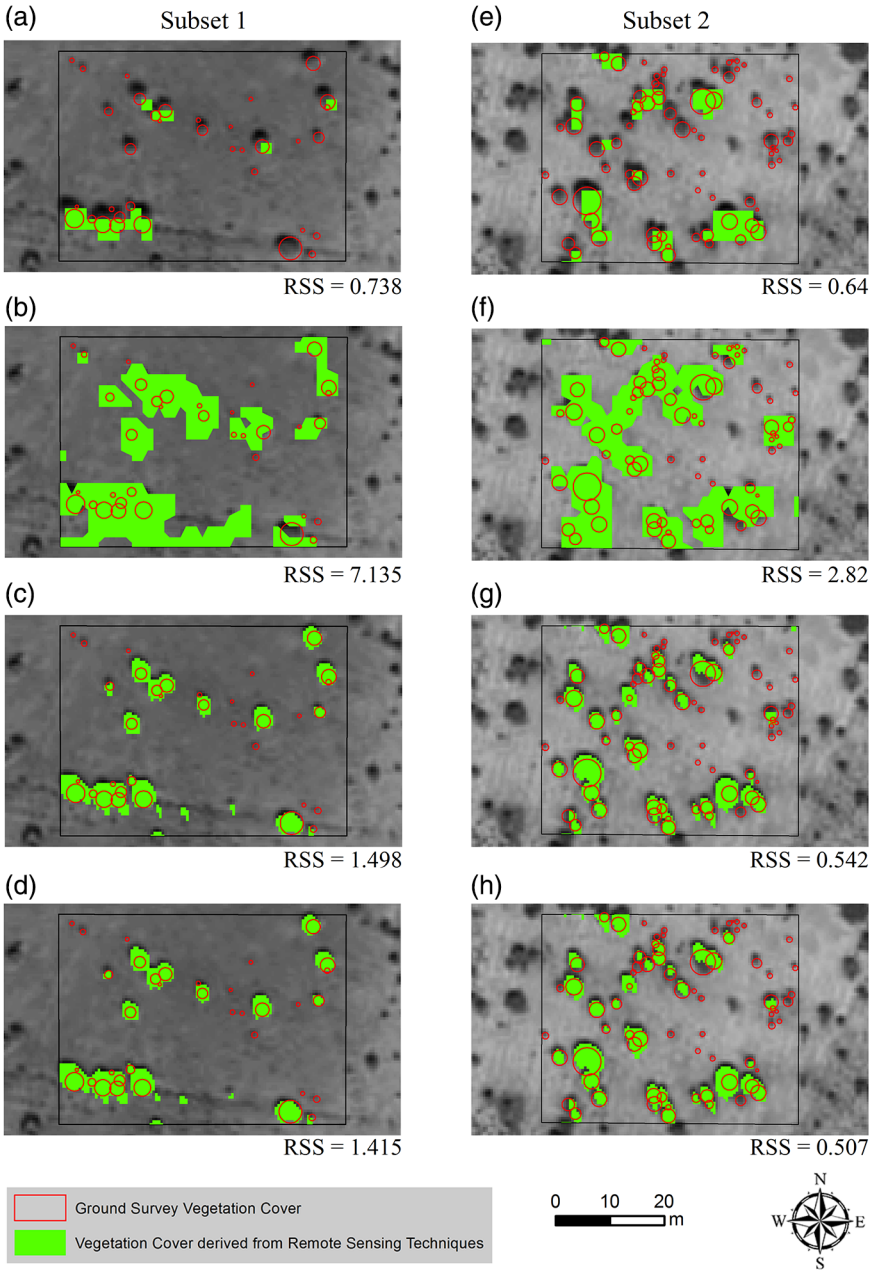

Fig. 6 Vegetation-cover outputs for the different approaches undertaken in this study. Subset 1: (a) optimum threshold MSAVI-2 (0.24), (b) IMAGINE Objective Threshold and Clump with Shadow Association, (c) VSM-1, and (d) VSM-2. Subset 2: (e) optimum threshold NDVI (0.3), (f) IMAGINE Objective Threshold and Clump with Shadow Association, (g) VSM-1, and (h) VSM-2.

VSM-2 was able to detect individual shrubs and trees in an arid environment, information that is rarely extracted using conventional remote-sensing methods. The use of shadow as a contextual reclassifier gives an extra advantage in the mapping approach, where it reduces the reliability on spectral information which can be a challenge for vegetation in desert environments. The benefit of VSM-2 is that it partially embraces conventional methods, such as VIs, that are most commonly used in vegetation monitoring and assessment, and adds an OBIA approach to further refine the results. On the other hand, there are several challenges within VSM-2 that should be taken into account: (1) the use of panchromatic imagery requires heavier computer processing, which may present challenges in operational use over large areas; (2) in certain locations and times, the sensor look angle could potentially lead to shadow occlusion by the shrubs and trees that generated them; thus, the VSM-2 model could be developed further to incorporate the full three-dimensional (3-D) geometry of Sun, satellite, sensor, location, and time; (3) topographic shadow presents a limitation where 3-D geometry of Sun, satellite, topography, and the object of interest should be taken into account; and (4) the usefulness of VSM-2 is yet to be tested at different locations and with satellite imagery such as GeoEye and Worldview 2/3.

The technique was solely designed to detect small- to large-sized arid shrubs and trees that are sparsely distributed and in fairly flat areas. When VSM-1 and VSM-2 were applied to the whole of the Pleiades satellite image, larger trees located in higher slopes returned higher coverage than the actual truth when visually interpreting the image and were unsuccessful in returning individual tree objects, resulting in an overclassified large patch of vegetation cover. VSM-1 and VSM-2 assumes a generally flat earth and shadows are projected onto the terrain which is flat or near flat. An issue that may be encountered is with steeper slopes that are oriented away from the Sun; these slopes will generate longer shadows than for flat ground and will lead to an over estimation and may also lead to overlap of shadows with adjacent trees. On the other hand, steeper slopes oriented toward the Sun will reduce the length of shadows and lead to under estimation. Moreover, higher density of shrubs and trees presents another problem where in the case of trees being close together, the shadow of one tree may fall on the next tree presenting a difficulty in separating tree objects. Correction techniques could consist of a modification of VSM-2 to account for terrain slope in the direction of Sun shadow; clearly, this would require the use of a digital elevation model at sufficient resolution to predict impacts of slope on shadow length.

Additional information that may be exploited in further development of VSM-2 includes the convolution values retained when applying the filter. Such information presents clues on the structural characteristics of the desert shrub. In addition to generic information, such as size classification of small, medium, and large, which is already complementary to the conventional assessment of vegetation cover in desert environments; potential use of the convolution values may present additional information on tree crown structure that can benefit ecological and landscape analysis of desert environments.

4 Conclusions

The limitations of classical VIs in mapping arid shrubs and trees invites investigation into creating improved methods and vegetation-cover extraction approaches. The results in this study suggests that an approach that combines VIs and OBIA can attain better results than just using classical VIs. Therefore, such efforts should be considered when extracting vegetation-cover parameters to input into desertification models. This study presented the VSM-2 approach that utilizes multiple filter sizes with promising results, demonstrating a statistical and visual improvement in comparison to VIs and the prebuilt IMAGINE Objective and eCognition object-oriented software. Potential avenues of improvement is the statistical evaluation of distributional accuracy to support the improvement observed in visual analysis and increase the confidence in the application of VSM-2. Instead of solely utilizing percent cover as employed in most remote-sensing studies, the RSS was used in assessing the performance of vegetation-cover classification integrating error metrics, which included commission and omission. The metric could be further developed to integrate an additional error metric such a distribution. In this study, we introduced a mechanism that can be used to investigate the best threshold and

best index using ground truth. This study has also identified that high-quality ground truth is required for achievement of best index thresholds. When this ground truth data is not available, the accuracy of the using VIs is less reliable. Further research could take into account the convolved values that are returned when applying the filter to the shadow image. Such values may give clues to structural information on the vegetation and should be further investigated and possibly integrated into the VSM.

The ability to detect individual desert shrubs and trees is promising when compared to conventional remote-sensing techniques that mostly extract generic vegetation cover. The VSM-2 approach provides encouraging opportunities for image processing associated with the increased presence of high-spatial resolution satellites and faster computer-processing capabilities. Not only will we be able to design an operational process that can detect vegetation cover in remote desert locations but also we will potentially be capable to extract extra information on individual shrubs and trees and their structural characteristics, and eventually extend such analysis to biomass estimation. Such information is vital for specialists (ecologist and rangeland managers) studying these type of environments.

Acknowledgments

We gratefully acknowledge Astrium/Airbus for providing the Pleiades satellite imagery and Ecole Nationale d'Agriculture de Meknes for their support in the field work. We also thank the University of South Australia for a travel grant, which provided logistical support for field work.

References

1. A. Roeder and J. Hill, *Recent Advances in Remote Sensing and Geoinformation Processing for Land Degradation Assessment*, CRC Press, United Kingdom (2009).
2. J. Hill et al., "Remote sensing and geomatics applications for desertification and land degradation monitoring and assessment," in *Geometrics for Land and Water Management: Achievements and Challenges in the Euromed Context, Int. Workshop*, R. Escadafal and M. L. Paracchini, Eds., pp. 15–22, Joint Research Centre, Italy (2004).
3. C. Leprieur et al., "Monitoring vegetation cover across semi-arid regions: comparison of remote observations from various scales," *Int. J. Remote Sens.* **21**(2), 281–300 (2000).
4. S. L. Ustin et al., "Remote sensing based assessment of biophysical indicators for land degradation and desertification," in *Recent Advances in Remote Sensing and Geoinformation Processing for Land Degradation Assessment*, A. Roeder and J. Hill, Eds., pp. 15–39, CRC Press, United Kingdom (2009).
5. G. Metternicht et al., "Remote sensing of land degradation: experiences from Latin America and the Caribbean," *J. Environ. Qual.* **39**(1), 42–61 (2009).
6. G. P. Asner and K. B. Heidebrecht, "Spectral unmixing of vegetation, soil and dry carbon cover in arid regions: comparing multispectral and hyperspectral observations," *Int. J. Remote Sens.* **23**(19), 3939–3958, (2002).
7. M. Dawelbait and F. Morari, "Monitoring desertification in a Savannah region in Sudan using Landsat images and spectral mixture analysis," *J. Arid. Environ.* **80**, 45–55, (2012).
8. J. Yang et al., "Landsat remote sensing approaches for monitoring long-term tree cover dynamics in semi-arid woodlands: comparison of vegetation indices and spectral mixture analysis," *Remote Sens. Environ.* **119**, 62–71, (2012).
9. M. Stellmes et al., "Dryland observation at local and regional scale—comparison of Landsat TM/ETM+ and NOAA AVHRR time series," *Remote Sens. Environ.* **114**(10), 2111–2125, (2010).
10. T. Blashcke and J. Strobl, "What's wrong with pixels?," *GIS-Zeitschrift für Geoinf. Syst.* **14**(6), 12–17 (2001).
11. S. Bernabé et al., "Spectral unmixing of multispectral satellite images with dimensionality expansion using morphological profiles," *Proc. SPIE* **8514**, 85140Z (2012).
12. N. B. Mishra and K. A. Crews, "Estimating fractional land cover in semi-arid central Kalahari: the impact of mapping method (spectral unmixing versus object based image analysis) and vegetation morphology." *Geocarto Int.* **29**(8), 860–877 (2014).

13. N. B. Mishra and K. A. Crews, "Mapping vegetation morphology types in a dry savanna ecosystem: integrating hierarchical object-based image analysis with random forest," *Int. J. Remote Sens.* **35**(3), 1175–1198 (2014).
14. T. Blaschke et al., "Geographic object-based image analysis—towards a new paradigm," *ISPRS J. Photogramm. Remote Sens.* **87**, 180–191, (2014).
15. E. Chuveico and A. Huete, *Fundamentals of Satellite Remote Sensing*, CRC Press, United Kingdom (2010).
16. T. Blaschke, "Object based image analysis for remote sensing," *ISPRS J. Photogramm. Remote Sens.* **65**(1), 2–16 (2010).
17. S. Alsharrah et al., "High-spatial resolution multispectral and panchromatic satellite imagery for mapping perennial desert plants," *Proc. SPIE* **9644**, 96440Z (2015).
18. R. Ritcher, "ATCOR for IMAGINE 2015," Geosystems GmbH, Wesslings, Germany (2015).
19. T. S. Purevdorj et al., "Relationships between percent vegetation cover and vegetation indices," *Int. J. Remote Sens.* **19**(18), 3519–3535 (1998).
20. A. Elmore et al., "Quantifying vegetation change in semiarid environments," *Remote Sens. Environ.* **73**(1), 87–102 (2000).
21. S. Barati et al., "Comparison the accuracies of different spectral indices for estimation of vegetation cover fraction in sparse vegetated areas," *Egypt. J. Remote Sens. Space Sci.* **14**(1), 49–56 (2011).
22. F. Gougeon and D. Leckie, "Forest information extraction from high spatial resolution images using an individual tree crown approach," Natural Resources Canada, Victoria, British Columbia, Information report [BC-X series] (2003).
23. D. S. Culvenor, "TIDA: an algorithm for the delineation of tree crowns in high spatial resolution remotely sensed imagery," *Comput. Geosci.* **28**(1), 33–44, (2002).
24. J. W. Rouse et al., "Monitoring the vernal advancement and retrogradation (greenware effect) of natural vegetation," NASA/GSFCT, Greenbelt, Maryland, Type 3, Final Report (1974).
25. A. R. Huete, "A soil-adjusted vegetation index (SAVI)," *Remote Sens. Environ.* **25**(3), 295–309 (1988).
26. J. Qi et al., "A modified soil adjusted vegetation index," *Remote Sens. Environ.* **48**(2), 119–126 (1994).
27. F. Baret and G. Guyot, "Potentials and limits of vegetation indices for LAI and APAR assessment," *Remote Sens. Environ.* **35**, 161–173 (1991).
28. C. Perry and L. Lautenschlager, "Functional equivalence of spectral vegetation indices," *Remote Sens. Environ.* **14**(1-3), 169–182 (1984).
29. G. Pickup et al., "Estimating the changes in vegetation cover over time in arid rangelands using Landsat MSS data," *Remote Sens. Environ.* **43**, 243–263 (1993).
30. Hexagon Geospatial, "ERDAS IMAGINE 2015," Norcross, Georgia (2015).
31. J. R. Jensen, *Introductory Digital Image Processing: A Remote Sensing Perspective*, Prentice Hall, Upper Saddle River, New Jersey (2005).
32. B. Herrera et al., "Automatic classification of trees outside forest using an object-driven approach: an application in a Costa Rican landscape," *Photogramm. Fernerkundung Geoinf.* **8**(2), 111–119 (2004).
33. G. Mallinis et al., "Object-based classification using quickbird imagery for delineating forest vegetation polygons in a Mediterranean test site," *ISPRS J. Photogramm. Remote Sens.* **63**(2), 237–250 (2008).
34. C. Pascual et al., "Object-based semi-automatic approach for forest structure characterization using Lidar data in heterogeneous Pinus sylvestris stands," *For. Ecol. Manage.* **255**(11), 3677–3685 (2008).
35. L. K. Dorren et al., "Improved Landsat-based forest mapping in steep mountainous terrain using object-based classification," *For. Ecol. Manage.* **183**(1-3), 31–46 (2003).
36. P. Gartner et al., "Object based change detection of Central Asian Tugai vegetation with very high spatial resolution satellite imagery," *Int. J. Appl. Earth Obs. Geoinf.* **31**, 110–121 (2014).

37. A. S. Laliberte et al., "Object-oriented image analysis for mapping shrub encroachment from 1937 to 2003 in southern New Mexico," *Remote Sens. Environ.* **93**(1–2), 198–210, (2004).
38. A. S. Laliberte et al., "Multi-scale, object-oriented analysis of QuickBird imagery for determining percent cover in arid land vegetation," in *20th Biennial Workshop on Aerial Photography, Videography, and High Resolution Digital Imagery for Resource Assessment*, pp. 116–123, American Society for Photogrammetry and Remote Sensing, Texas (2005).
39. A. S. Laliberte et al., "Combining decision trees with hierarchical object-oriented image analysis for mapping arid rangelands," *Photogramm. Eng. Remote Sens.* **73**(2), 197–207, (2007).
40. M. Baatz and A. Schäpe, "Multiresolution segmentation: an optimization approach for high quality multi-scale image segmentation," in *Angewandte Geographische Inf. Verarbeitung XII*, J. Strobl et al., Eds., pp. 12–23, Wichmann Verlag, Heidelberg, Germany (2000).
41. U. C. Benz et al., "Multi-resolution, object-oriented fuzzy analysis of remote sensing data for GIS-ready information," *ISPRS J. Photogramm. Remote Sens.* **58**(3–4), 239–258, (2004).
42. T. Blaschke et al., "Multi-scale image analysis for ecological monitoring of heterogeneous, small structured landscapes," *Proc. SPIE* **4545**, 35 (2002).
43. C. Burnett and T. Blaschke, "A multi-scale segmentation/object relationship modelling methodology for landscape analysis," *Ecol. Model.* **168**(3), 233–249, (2003).

Saad A. Alsharrah received his bachelor's degree in geographic information systems and his master's degree in environmental management and sustainability from the University of South Australia, Australia, in 2009 and 2011, respectively. He is a PhD candidate at the Department of Natural and Built Environments, University of South Australia. His research interests include land degradation assessment and use of remote sensing for detection of vegetation cover in arid environments.

Rachid Bouabid received his PhD. He is a soil scientist. Currently, he is a professor at the Department of Soil Sciences, National School of Agriculture, Meknes, Morocco. He has teaching, research, and outreach responsibilities. His research interests include management of soil fertility and crop fertilization, mainly for orchards, soil conservation, GIS, and remote sensing. He is involved in several projects dealing with agriculture and rural development in various parts of Morocco.

David A. Bruce is an associate head at the School of Natural and Built Environments, University of South Australia. He has a long career in remote sensing and geographical information science in both government and academia; in the latter, he has taught at the undergraduate and postgraduate levels, supervises PhD students and undertakes research, which is currently focused in the analysis of high-spatial resolution satellite multispectral and multipolarimetric SAR images for environmental applications.

Sekhar Somenahalli currently teaches courses related to GIS and its applications to environment and planning disciplines in the School of Natural and Built Environments, University of South Australia, Adelaide. He is an expert in GIS applications and has over 20 years of teaching, research, and industry experience. He has extensively researched and published more than 60 refereed papers in journals and conferences, and has been invited to present his research at national and international levels.

Paul A. Corcoran joined the Ordnance Survey, Great Britain's national mapping agency in 1984 and undertook various surveying, GIS and management roles, predominantly in the North of England. In 2006, he joined the School of Natural and Built Environments, University of South Australia, Adelaide, as a geospatial science lecturer. In 2013, he became program director for the Bachelor of Environmental Science, Bachelor of Geospatial Science, and Master of Surveying.